BMC
Genomics

RESEARCH ARTICLE

Open Access

DNA methylation profile dynamics of tissue-dependent and differentially methylated regions during mouse brain development

Keiji Hirabayashi, Kunio Shiota and Shintaro Yagi[*]

Abstract

Background: Tissues and their component cells have unique DNA methylation profiles comprising DNA methylation patterns of tissue-dependent and differentially methylated regions (T-DMRs). Previous studies reported that DNA methylation plays crucial roles in cell differentiation and development. Here, we investigated the genome-wide DNA methylation profiles of mouse neural progenitors derived from different developmental stages using HpyCH4IV, a methylation-sensitive restriction enzyme that recognizes ACGT residues, which are uniformly distributed across the genome.

Results: Using a microarray-based genome-wide DNA methylation analysis system focusing on 8.5-kb regions around transcription start sites (TSSs), we analyzed the DNA methylation profiles of mouse neurospheres derived from telencephalons at embryonic days 11.5 (E11.5NSph) and 14.5 (E14.5NSph) and the adult brain (AdBr). We identified T-DMRs with different DNA methylation statuses between E11.5NSph and E14.5NSph at genes involved in neural development and/or associated with neurological disorders in humans, such as *Dclk1*, *Nrcam*, *Nfia*, and *Ntng1*. These T-DMRs were located not only within 2 kb but also distal (several kbs) from the TSSs, and those hypomethylated in E11.5NSph tended to be in CpG island (CGI-) associated genes. Most T-DMRs that were hypomethylated in neurospheres were also hypomethylated in the AdBr. Interestingly, among the T-DMRs hypomethylated in the progenitors, there were T-DMRs that were hypermethylated in the AdBr. Although certain genes, including *Ntng1*, had hypermethylated T-DMRs 5′ upstream, we identified hypomethylated T-DMRs in the AdBr, 3′ downstream from their TSSs. This observation could explain why *Ntng1* was highly expressed in the AdBr despite upstream hypermethylation.

Conclusion: Mouse adult brain DNA methylation and gene expression profiles could be attributed to developmental dynamics of T-DMRs in neural-related genes.

Keywords: DNA methylation, Tissue-dependent and differentially methylated region, Neural progenitor cells

Background

The adult mouse brain consists of various kinds of cells that sequentially appear as neurons, astrocytes, and oligodendrocytes from late gestation through the neonatal period. Distinctive neural progenitor cells (NPCs) that exhibit different differentiation potentials to neurons and glial cells are generated during mid-to-late gestation [1-3]. This process is controlled by signaling pathways composed of transcription factors; dysfunction in genes encoding these factors is known to result in brain malformation [4-6].

Epigenetic systems underlie the network of tissue- and developmental stage-specific transcription factors and their targets [7]. Major players in epigenetic systems are DNA methylation and histone modifications, which occur on nucleosomes and affect chromosomal activity by changing nucleosome architecture. Tissue-dependent and differentially methylated regions (T-DMRs) are found throughout the genome and influence tissue-specific gene expression. T-DMRs have been found 3′ downstream of transcription start sites (TSSs) in addition to in 5′-upstream promoter regions. A distinct combination of DNA methylation

* Correspondence: asyagi@mail.ecc.u-tokyo.ac.jp
Laboratory of Cellular Biochemistry, Department of Animal Resource Sciences/Veterinary Medical Sciences, The University of Tokyo, Yayoi 1-1-1, Bunkyo-ku, Tokyo 113-8657, Japan
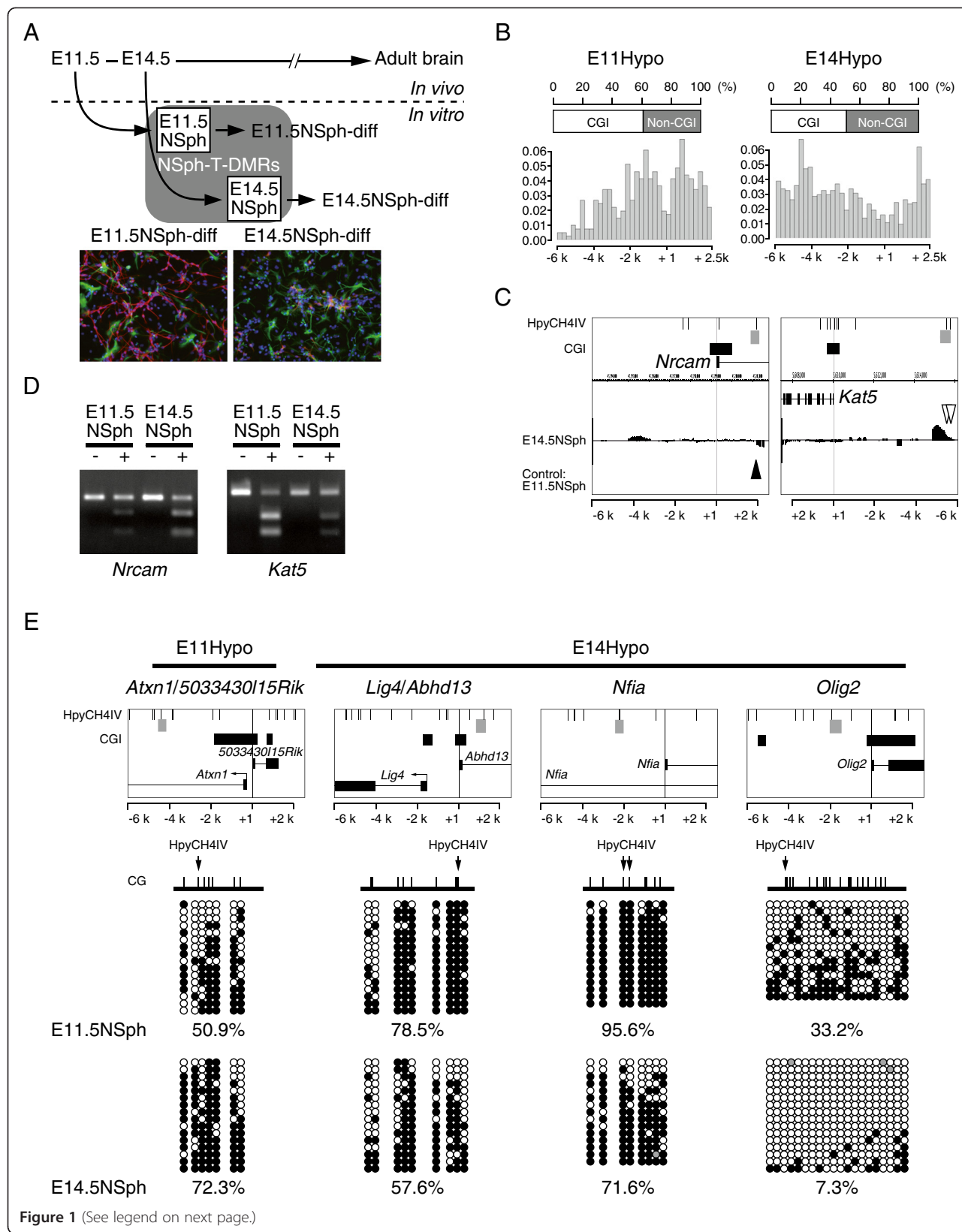
Figure 1 (See legend on next page.)

(See figure on previous page.)
Figure 1 Distinct DNA methylation profile between E11.5NSph and E14.5NSph. (A) Schematic of the analysis in this study. E11.5NSph and E14.5NSph were cultured from telencephalons of E11.5 and E14.5 mouse embryos and used as models of NPCs. Comparative analysis of D-REAM data was performed to identify NSph-T-DMRs. Immunocytochemical analysis of differentiated NSphs (E11.5NSph-diff and E14.5NSph-diff) was conducted using antibodies against βIII-tubulin (TUBB3) and glial fibrillary acidic protein (GFAP). TUBB3-positive and GFAP-positive cells are indicated in red and green, respectively, and DAPI-stained nuclei are indicated in blue. **(B)** Distinct characteristics of E11Hypo-T-DMRs and E14Hypo-T-DMRs. The proportion of CGI genes (upper bar charts) and the distributions of NSph-T-DMRs to TSSs (lower panels) are displayed. E11Hypo-T-DMRs (left) and E14Hypo-T-DMRs (right) were mapped in 208 and 604 genes, respectively. The y-axis represents the proportions of each fraction to the whole as 1. The width of the histogram is 250 bp. **(C)** Integrated Genome Browser (IGB) images of *Nrcam* and *Kat5* gene loci (Ensembl Transcripts) showing comparative MATscores of E14.5NSph to E11.5NSph. Filled and open arrowheads indicate E11Hypo-T-DMRs and E14Hypo-T-DMRs, respectively. Regions analyzed by COBRA (D) are represented by gray rectangles. **(D)** COBRA representing DNA methylation status of HpyCH4IV sites in *Nrcam* and *Kat5* gene regions. Bisulfite PCR products using genomic DNA from E11.5NSph and E14.5NSph were not treated (−) or treated with HpyCH4IV (+) and electrophoresed. **(E)** DNA methylation status of the indicated regions located in 4 disease-associated genes (gray rectangles of the upper panels) was analyzed by bisulfite sequencing. Each open, filled, and gray circle represents unmethylated, methylated CpG, and CpG with an undetermined methylation state, respectively. Percentages of methylated CpGs are indicated.

patterns at T-DMRs determines cellular identity during development [8-13], thus illustrating that DNA methylation profiles are unique to individual cells or tissue types [7,14,15].

Genome-wide DNA methylation analyses focusing on proximal promoter regions in embryonic stem cell-derived NPCs and NPCs committed to astrocytes indicate the importance of DNA methylation in the commitment process and differentiation potential of NPCs [16-19]. These reports indicated that the majority of DNA methylation changes occur at low-CpG density promoters, suggesting sequence preferences in DNA methylation targets during neural differentiation [18]. However, T-DMRs are observed at high-CpG density promoters, such as those containing CpG islands (CGIs), and are tissue-dependently methylated in the adult brain (AdBr) [7,20].

In this study, we performed a comparative analysis of DNA methylation status in NPCs derived from mid- and late-gestation mouse embryo. Using microarray-based, genome-wide DNA methylation profiling [7], we identified T-DMRs in dozens of genes, and we illustrate dynamic DNA methylation statuses for dozens of T-DMRs, which are reflected in the DNA methylation profile of the AdBr.

Results
Distinct DNA methylation profiles in NPCs with different fates
To explore DNA methylation profiles of mouse NPCs, we compared neurospheres (NSph) derived from telencephalons at embryonic days 11.5 (E11.5NSph) and 14.5 (E14.5NSph) by T-DMR profiling with restriction tag-mediated amplification (D-REAM) with mouse promoter tiling arrays covering from 6 kb upstream to 2.5 kb downstream of 30,140 gene TSSs (Ensembl Transcript IDs) [7]. The distinctive cell fates of E11.5NSph and E14.5NSph were indicated by biased expression of marker genes for neural and oligodendrocyte progenitor

in the undifferentiated NSph, and those of neuronal and glial marker genes in the differentiated ones, respectively (Figure 1A and Additional file 1: Figure S1). We screened genomic regions that exhibited differential MATscores [7,21] between NSphs, which indicate differential methylation status, and obtained a total of 1,403 NSph-T-DMRs consisting of 380 E11Hypo-T-DMRs and 1,023 E14Hypo-T-DMRs, which were hyper- and hypomethylated, respectively, in E14.5NSph compared to E11.5NSph.

The localization patterns along the genome were distinct between E11Hypo-T-DMRs and E14Hypo-T-DMRs. The former exhibited bimodal distributions within 2.5 kb from TSSs and biased to the CGI genes, which contain CGIs around TSSs [7]; the latter were located 6 kb to 2 kb upstream of TSSs without any promoter type bias (Figure 1B). These findings are noteworthy because they indicate that methylation changes occur in regions around high-CpG promoters. We analyzed E11Hypo-T-DMR 3′ downstream from the *Nrcam* TSS, and E14Hypo-T-DMR 5′ upstream from the *Kat5* TSS. Combined bisulfite restriction analysis (COBRA) of these T-DMRs indicated differential DNA methylation status as indicated by D-REAM (Figure 1C and 1D).

Among the genes with NSph-T-DMRs, we identified human gene orthologs involved in neurological diseases, such as spinocerebellar ataxia type 1 (*ATXN1* and *KAT5*), schizophrenia (*BLOC1S1*, *NTNG1*, and *OLIG2*), autism (*NRCAM*), and brain malformation syndrome (*LIG4* and *NFIA*) (Additional file 2: Table S1). We performed bisulfite sequencing of 1 E11Hypo-T-DMR (*Atxn1*) and 3 E14Hypo-T-DMRs (*Lig4*, *Nfia*, and *Olig2*) that were located at various relative positions from the TSSs, including one associated with an alternative TSS and those facing their TSS in proximal regions. The results showed clear differences in the DNA methylation statuses of CpG sites around the HpyCH4IV sites between the 2 types of NSphs (Figure 1E). These data indicate that methylation changes occurred in a subpopulation of NSphs in a gene-dependent manner.

Association of NSph-T-DMRs with neural development and function

We performed gene ontology (GO) analysis to characterize genes with the NSph-T-DMRs. The neural-related GO term "central nervous system development" was enriched in genes with E11Hypo-T-DMRs but was not enriched in those with E14Hypo-T-DMRs (Tables 1 and 2). Genes with E11Hypo-T-DMRs included those for neuronal differentiation and functions: specification of retinal amacrine neurons (*Barhl2*), axon outgrowth (*Dclk1*), inhibition of oligodendrocyte differentiation (*Id2*), and axon guidance (*B3gnt2* and *Nrcam*). Among genes with E14Hypo-T-DMRs, we found those involved in astrocyte and/or oligodendrocyte development, such as *Nfia* and *Olig2*. Both E11Hypo- and E14Hypo-T-DMR genes included those involved in cell fate commitment (*Barhl2*, *Olig2*, and *Cdon*) and brain morphogenesis (*Tcfap2a*, *Fezf1*, *Cer1*, and *Cdon*). A search of the OMIM (Online Mendelian Inheritance in Man) database indicated that genes with E14Hypo-T-DMRs that encode membrane-associated proteins (*Accn1*, *Scg5*, and *Slc15a2*) are expressed in the AdBr (Table 2). Thus, developmental stage-specific methylation and demethylation at the T-DMRs in genes related to neuronal and glial development occurred during neural cell fate determination.

DNA methylation profile of NSph-T-DMRs in the AdBr

We compared D-REAM data between NSphs and the AdBr and used K-means clustering to classify E11hypo- and E14hypo-T-DMRs into 3 clusters. In the AdBr, most E11Hypo-T-DMRs and E14Hypo-T-DMRs exhibited hypomethylation (clusters 2 and 3) (Figure 2A). Although the degrees of differences varied among genes, COBRA of NSph-T-DMRs indicated hypomethylated status at some loci as clusters 2 and 3 (e.g., *Dclk1* and *B3gnt2* for E11Hypo-TDMR, and *Rdh5*/*Bloc1s1* and *Mcf2l* for E14Hypo-T-DMRs), and hypermethylated status at other loci as cluster 1 (e.g., *Cdkn2a* and *Ntng1* for E11Hypo- and E14Hypo-T-DMRs, respectively) in the

AdBr (Figure 2B and Additional files 3 and 4: Tables S2 and S3).

Among genes with cluster-1 E14Hypo-T-DMRs, we unexpectedly found that T-DMR hypermethylation was associated with higher gene expression in the brain (described later). To address this issue, we further investigated the DNA methylation status of other HpyCH4IV sites in these genes using AdBr D-REAM data and found AdBr-specific hypomethylated T-DMRs 3′ downstream of their TSSs in *Ntng1*, *Aldh1a2*, and *Accn1* (Figure 3A). It is noteworthy that all these T-DMRs were located within few kb from CGIs.

The positional changes of hypomethylated T-DMRs in a specific genomic region are summarized in Figure 3B. Bisulfite sequencing analysis of T-DMRs in the *Ntng1* gene indicated hypermethylation of E14Hypo-T-DMRs at the 5′-upstream region and hypomethylation at the 3′ downstream of the TSS in the AdBr with unmethylated neighboring regions in all samples (Figure 3C). Quantitative reverse-transcription polymerase chain reaction (Q-RT-PCR) data indicated negative correlation between hypomethylation at distal T-DMR (region 4) in undifferentiated NSphs, and an association of gene expression in AdBr with hypomethylation of the T-DMR 3′ downstream of the CGI (Figure 3D). These results highlight functions associated with developmental stage-dependent multiple T-DMRs in a gene region.

Discussion

Comparing NSphs with different cell fates enabled the identification of numerous T-DMRs in genes at different relative positions from TSSs. DNA methylation and demethylation occurred in a developmental stage-dependent manner, and changes in DNA methylation at these T-DMRs resulted in variable methylation in AdBr cells that shifted the DNA methylation profile as a whole. The hypomethylated status of most NSph-T-DMRs was reflected in the DNA methylation profile of the AdBr to different degrees in a locus-specific manner. The previous genome-wide methylation analyses of NPCs [16-18] emphasized preexisting epigenetic marks, such as bivalent histone modifications on poised genes involved in early differentiation processes and demethylated promoters of astrocyte-specific genes in progenitor cells preceding expression in differentiated cells. DNA methylation status in NSphs and gene expression in the AdBr have led to the hypothesis that a considerable number of T-DMRs identified in this study are epigenetically marked prior to gene expression. The developmental-stage specific DNA methylation marks could be useful for identify and evaluation of NPCs established from not only fetus but also stem cells as pluripotent stem cells and those from adult tissues.

Table 1 Annotation analysis of genes with NSph-T-DMRs

Category	Term	P value
Genes with E11Hypo-T-DMRs		
BP	Central nervous system development	1.01E-02
MF	Cyclin-dependent protein kinase inhibitor activity	1.57E-03
KEGG	Propanoate metabolism	1.40E-03
Genes with E14Hypo-T-DMRs		
BP	Positive regulation of developmental process	8.08E-03
CC	Peroxisome	7.43E-03
MF	Transmembrane transporter activity	1.41E-02
KEGG	Retinol metabolism	2.80E-03

BP, MF, KEGG, and CC indicate biological process, molecular function, KEGG pathway, and cellular component, respectively.

Table 2 Genes with NSph-T-DMRs annotated for neural development and functions

NSph-T-DMR	Gene	Description	GO terms related to development and neural functions	OMIM
E11Hypo	Atxn1	Ataxin 1	Transmission of nerve impulse	601556
E11Hypo	B3gnt2	UDP-GlcNAc:betaGal beta-1, 3-N-acetylglucosaminyltransferase 2	Ax, ND, sensory perception	605581
E11Hypo	Barhl2	BarH-like 2 (Drosophila)	Ax, CC, ND	605212
E11Hypo	Cdkn2a	Cyclin-dependent kinase inhibitor 2A		600160
E11Hypo	Dclk1	Doublecortin-like kinase 1	Ax, ND	604742
E11Hypo	Id2	Inhibitor of DNA binding 2		600386
E11Hypo	Nrcam	Neuron-glia-CAM-related cell adhesion molecule	Ax, ND, transmission of nerve impulse	601581
E11Hypo	Tcfap2a	Transcription factor AP-2, alpha	neural tube closure	107580
E11Hypo/E14Hypo	Cer1	Cerberus 1 homolog (Xenopus laevis)		603777
E14Hypo	Accn1	Amiloride-sensitive cation channel 1, neuronal (degenerin)	Sensory perception	601784
E14Hypo	Aldh1a2	Aldehyde dehydrogenase family 1, subfamily A2	ND	603687
E14Hypo	Atp11a	ATPase, class VI, type 11A		605868
E14Hypo	Bloc1s1	Biogenesis of lysosome-related organelles complex-1, subunit 1		601444
E14Hypo	Cdon	Cell adhesion molecule-related/down-regulated by oncogenes	CC	608707
E14Hypo	Dph5	DPH5 homolog (S. cerevisiae)		611075
E14Hypo	Emid1	EMI domain containing 1		608926
E14Hypo	Fezf1	Fez family zinc finger 1	Ax, ND	613301
E14Hypo	Kat5	K(lysine) acetyltransferase 5		601409
E14Hypo	Lig4	Ligase IV, DNA, ATP-dependent	Neuron apoptosis	601837
E14Hypo	Mcf2l	Mcf.2 transforming sequence-like		609499
E14Hypo	Nfia	Nuclear factor I/A		600727
E14Hypo	Ntng1	Netrin G1	Ax, ND	608818
E14Hypo	Olig2	Oligodendrocyte transcription factor 2	CC, ND, gliogenesis, transmission of nerve impulse	606386
E14Hypo	Scg5	Secretogranin V	Neuropeptide signaling pathway	173120
E14Hypo	Slc15a2	Solute carrier family 15 (H+/peptide transporter), member 2		602339
E14Hypo	Wasl	Wiskott-Aldrich syndrome-like (human)		605056

Ax, axonogenesis; CC, cell fate commitment; ND, neuron differentiation.

We observed developmental position changes such as 5′ distal hypomethylated T-DMRs in the NSphs and hypomethylated T-DMR marks 3′ proximal downstream of TSSs in the fully developed brain. These T-DMRs were often located around CGIs, which is in contrast to a previous genome-wide analysis of NPCs indicating biased DNA methylation changes to low-CpG promoters [17,18]. T-DMRs found in the *Ntng1* locus could be classified into the previously described class of T-DMRs downstream of TSSs of CGI genes, in which hypomethylation was well correlated with gene expression [7,20]. T-DMRs have been identified at the edges of CGIs [22], and DMRs around CGIs, named as CpG island shores, are identified in not only normal tissues but also cancer cells [23]. The biased distribution of E14Hypo-T-DMRs to the relatively 5′-distal positions from TSSs suggested that hypomethylation of these 5′-distal T-DMRs in the progenitor cells are epigenetic marks that lead to expression in differentiated cells, which exhibit hypomethylation of T-DMRs at 3′ downstream of TSS.

Systematic biases are inevitable for any genome-wide DNA methylation analysis: both Microarray-based Integrated Analysis of Methylation by Isoschizomers (MIAMI) [16] and Reduced Representation Bisulfite Sequencing (RRBS) [18], methods used in the previous epigenomic study in NPCs, are inevitably focusing on CGIs because of the biased distribution of MspI recognition sites that they uses for enrichment of fragments [24]; Methylated DNA
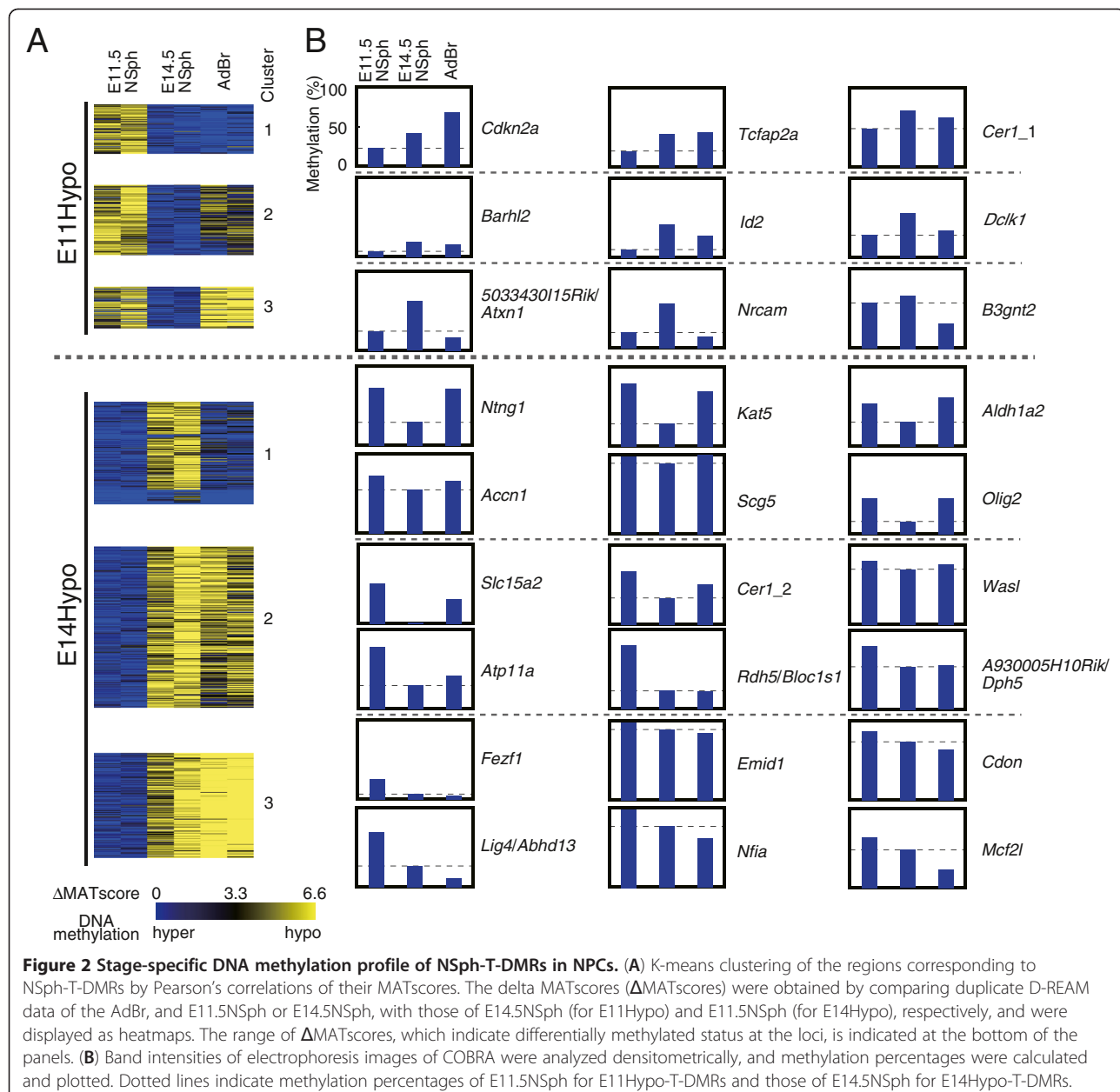
Figure 2 Stage-specific DNA methylation profile of NSph-T-DMRs in NPCs. (A) K-means clustering of the regions corresponding to NSph-T-DMRs by Pearson's correlations of their MATscores. The delta MATscores (ΔMATscores) were obtained by comparing duplicate D-REAM data of the AdBr, and E11.5NSph or E14.5NSph, with those of E14.5NSph (for E11Hypo) and E11.5NSph (for E14Hypo), respectively, and were displayed as heatmaps. The range of ΔMATscores, which indicate differentially methylated status at the loci, is indicated at the bottom of the panels. **(B)** Band intensities of electrophoresis images of COBRA were analyzed densitometrically, and methylation percentages were calculated and plotted. Dotted lines indicate methylation percentages of E11.5NSph for E11Hypo-T-DMRs and those of E14.5NSph for E14Hypo-T-DMRs.

immunoprecipitation (MeDIP) [17], is known to have bias to high density CpG promoter [25]. Approximately 50% of promoters are associated with CGIs. D-REAM also has [7,25]. Only limited numbers of genes are coincided to be predicted to have DMRs in NSph: *Gfap*, which have been shown to have DMR hypomethylated in E14.5NSph [18], was not included in our gene list because of lacking Hpy-CH4IV site in the proximal promoter region: DMRs on *Ntng1*, which was identified in this study, is an example of novel T-DMRs not described in the previous studies.

Several converging lines of evidence have indicated the significance of DNA methylation in normal brain function. Mutations in *Dnmt1*, *Dnmt3b*, and *Mecp2* result in

functional and/or morphological abnormalities in human and mouse brain [26-28]. Mutations in the human orthologs of some genes carrying NSph-T-DMR, such as *LIG4* and *NFIA*, are associated with neurological disorders [29,30]. Similar phenotypes are observed in mice harboring mutations in these genes [4,31]. Targeted mutation of 2 genes with E11Hypo-T-DMRs, *Dclk1* and *Nrcam*, results in axonal defects in mice [32,33]. Disorganized DNA methylation profiles have been reported in cloned animals [34], chemically treated cells [35], and in certain diseases [36,37]. Epimutations in tumor suppressor genes are involved in carcinogenesis [38]. Therefore, the establishment of DNA methylation status at T-
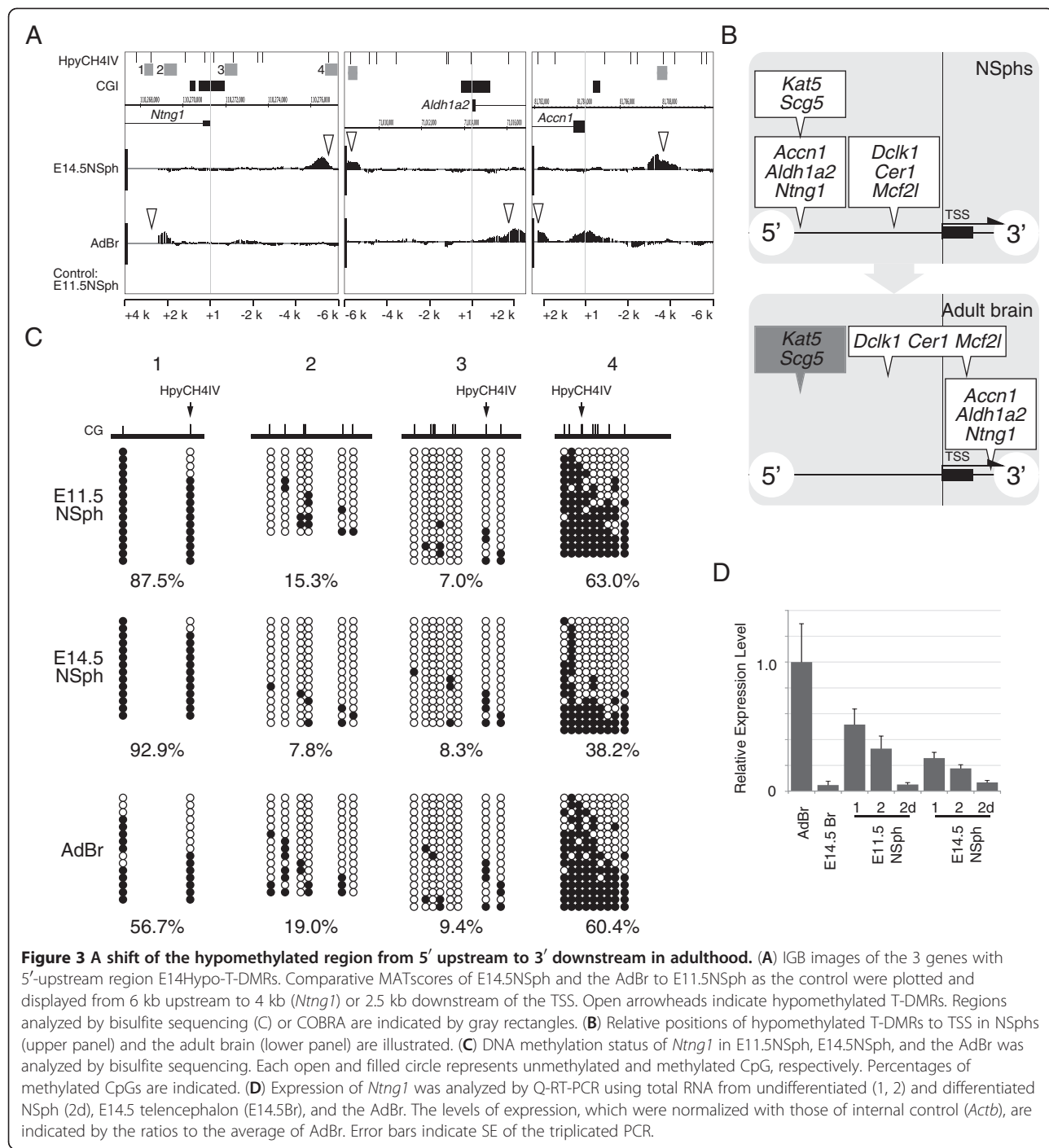
Figure 3 A shift of the hypomethylated region from 5′ upstream to 3′ downstream in adulthood. (**A**) IGB images of the 3 genes with 5′-upstream region E14Hypo-T-DMRs. Comparative MATscores of E14.5NSph and the AdBr to E11.5NSph as the control were plotted and displayed from 6 kb upstream to 4 kb (*Ntng1*) or 2.5 kb downstream of the TSS. Open arrowheads indicate hypomethylated T-DMRs. Regions analyzed by bisulfite sequencing (C) or COBRA are indicated by gray rectangles. (**B**) Relative positions of hypomethylated T-DMRs to TSS in NSphs (upper panel) and the adult brain (lower panel) are illustrated. (**C**) DNA methylation status of *Ntng1* in E11.5NSph, E14.5NSph, and the AdBr was analyzed by bisulfite sequencing. Each open and filled circle represents unmethylated and methylated CpG, respectively. Percentages of methylated CpGs are indicated. (**D**) Expression of *Ntng1* was analyzed by Q-RT-PCR using total RNA from undifferentiated (1, 2) and differentiated NSph (2d), E14.5 telencephalon (E14.5Br), and the AdBr. The levels of expression, which were normalized with those of internal control (*Actb*), are indicated by the ratios to the average of AdBr. Error bars indicate SE of the triplicated PCR.

DMRs in these genes indicates the possibility that epimutations at T-DMRs could be involved in neurological disorders without genetic alterations.

Conclusions

The dynamics of T-DMRs, several of which are often identified around TSS of a single gene during neural development, contribute regulation of developmental expression of genes and the DNA methylation profile of mouse adult brain. The identified T-DMRs could be used for evaluation and identification of NPCs, and for epimutation analysis in neural diseases.

Methods

Tissue samples, neurosphere culture, and immunocytochemistry

All experiments using mice were carried out according to the institutional guidelines for the care and use of

laboratory animals (Graduate School of Agricultural and Life Sciences, the University of Tokyo). Pregnant C57BL/6 N mice were euthanized, and fetuses were recovered in ice-cold phosphate-buffered saline (PBS) containing 0.6% glucose. For neurosphere culture, dissected telencephalons were dispersed, and were suspended in progenitor cell culture medium: Dulbecco's modified Eagle's medium (DMEM)/F12 (1:1) containing 5.5 mM HEPES, 2 mM L-glutamine, 1/50 volume of B-27 Supplement (Invitrogen), 20 ng/ml epidermal growth factor (EGF), 20 ng/ml human basic fibroblast growth factor (bFGF) (Pepro-Tech), and 5 μg/ml heparin. Cells were seeded into a petri dish and cultured for 6 days, replacing half of the medium with fresh medium at day 3. To induce differentiation, cells were dispersed, suspended in differentiation medium (progenitor cell culture medium without EGF, bFGF, and heparin), and seeded onto poly-L-lysine- and laminin-coated coverslips for immunocytochemistry. After 4 days of culture, cells were fixed with 4% paraformaldehyde and stained with a monoclonal antibody against βIII-tubulin (Covance) and a rabbit polyclonal antibody against glial fibrillary acidic protein (DAKO).

Genomic DNA extraction

Cells (1.5×10^6) were incubated in 200 μl of lysis solution (10 mM Tris–HCl (pH 8.0), 5 mM EDTA, 200 mM NaCl, 0.2% SDS and 200 μg/ml proteinase K) at 55°C for 30 min. The samples were extracted with phenol/chloroform/isoamyl alcohol (PCI; 25:24:1), incubated with RNase for 30 min, and extracted again with PCI. Genomic DNA was precipitated with ethanol and dissolved in 20 μl of TE (pH 8.0).

D-REAM

D-REAM was performed as previously described [7]. Genomic DNA (5 μg) was digested with HpyCH4IV (New England Biolabs), extracted with PCI and chloroform, ethanol-precipitated, and dissolved in TE (pH 8.0). DNA sample (50 ng) was ligated to the R-adaptor pair using T4 DNA ligase (New England Biolabs) at 16°C overnight. After the 5′-overhang of the adaptor was filled in with Klenow Fragment, the DNA was digested with TaqI at 65°C for at least 1 h and purified with a Micro-spin S-300 HR Column (GE Healthcare). The TaqI ends of the DNA were ligated to the N-adaptor pair. The resulting DNA sample was purified with the Wizard SV Gel and PCR Clean-up System (Promega) and amplified with the R18 and N18 primers and Immolase Taq DNA polymerase (Bioline) under the following conditions: denaturation at 95°C for 7 min, followed by 20 cycles of 30 sec at 95°C, 30 sec at 62°C, and 2 min at 72°C. DNA was purified with MinElute PCR Purification Kit (Qiagen), and 7.5 μg of DNA was used for microarray analysis. Microarray analysis was conducted with GeneChip

System (Affymetrix), and all procedures were done according to the Affymetrix Chromatin Immunoprecipitation Assay Protocol. DNA samples were labeled with the Gene-Chip WT Double-Stranded DNA Terminal Labeling Kit and hybridized with GeneChip Mouse Promoter 1.0R Arrays. Arrays were stained and washed with GeneChip Fluidics Station 450 and scanned with GeneChip Scanner 3000 7 G. The instruments were operated with GeneChip Operating Software version 1.4. D-REAM data obtained in this study have been deposited in the ArrayExpress database (accession number E-MTAB-1150). The D-REAM dataset of the adult whole cerebrums (AdBr), which were obtained from 13 week-old male mice, is reported previously [7].

Data analysis

D-REAM data for two experiments were obtained for each NSph. The data were visualized using the Integrated Genome Browser (Affymetrix). Ensembl Transcript IDs (release 46) associated with T-DMR were obtained using BioMart [39] and Galaxy website [40]. Distribution analysis was conducted with the R software package. K-means clustering of MATscores was performed with the MultiExperiment Viewer (MeV in TM4 Microarray Software Suite) [41]. Gene Ontology analysis was conducted using the DAVID Bioinformatics Resources website [42].

Combined bisulfite restriction analysis (COBRA) and sequencing

PstI- or EcoRV-digested genomic DNA (3 μg) was denatured with 0.3 M NaOH. Sodium metabisulfite (pH 5.0) and hydroquinone were added to final concentrations of 2.0 M and 0.5 mM, respectively. The reaction mixtures were incubated in the dark at 55°C for 16 h. The DNA was purified with the Wizard DNA Clean-up System (Promega), treated with 0.3 M NaOH at 37°C for 15 min, and ethanol-precipitated. The DNA was dissolved in 20 μl of TE (pH 8.0). After the bisulfite reaction, the unmethylated CpGs are converted to uracil-phosphate-guanines (UpGs), whereas the methylated CpGs remain intact. One-hundredth to 1/20 amount of the DNA was used for PCR with Immolase Taq DNA polymerase. For COBRA, one-tenth of the PCR product was digested with HpyCH4IV at 37°C overnight and electrophoresed with untreated control in a 2% agarose gel. For sequencing, PCR product was purified with the Wizard SV Gel and PCR Clean-up System (Promega) and cloned into pGEM-T Easy Vector (Promega). Up to 16 clones were sequenced. Primer sets used are listed in Additional file 5: Table S2.

RT-PCR

Total RNA was extracted with the TRIzol Reagent (Invitrogen), and 1 μg of total RNA was subjected to reverse

transcription using the Superscript II First-strand Synthesis System (Invitrogen). One-hundredth of the cDNA was used for PCR with Immolase Taq DNA polymerase under the following conditions: denaturation at 95°C for 7 min and 23 or 35 cycles of 30 sec at 95°C, 30 sec at 62°C, and 30 sec at 72°C (Additional file 5: Table S2). Quantitative RT-PCR was carried-out on Bio-Mark HD system (Fluidigm) using Universal probes (Roche Applied Science) for monitoring amplifications (detailed in Additional file 6). Makers were selected according to the previous report [43].

Additional files

Additional file 1: Figure S1. NSph differentiation capacity.

Additional file 2: Table S1. Associations of genes carrying NSph-T-DMRs with human neurological disease.

Additional file 3: Figure S2. Integrated Genome Browser (IGB) images of the genes (Ensembl Transcripts) with E11Hypo- (A) and E14Hypo-T-DMRs (B).

Additional file 4: Figure S3. COBRA representing DNA methylation status of NSph-T-DMRs.

Additional file 5: Table S2. Primers used in this study.

Additional file 6: Method and Primer list for Q-RT-PCR.

Abbreviations
T-DMRs: Tissue-dependent and differentially methylated regions; TSSs: Transcription start sites; AdBr: Adult brain; CGIs: CpG islands; NPCs: Neural progenitor cells; NSph: Neurospheres; D-REAM: T-DMR profiling with restriction tag-mediated amplification; COBRA: Combined bisulfite restriction analysis; GO: Gene ontology; Q-RT-PCR: Quantitative reverse-transcription polymerase chain reaction.

Competing interests
The authors declare no conflicts of interest.

Authors' contributions
KH, KS and SY designed this study. KH and SY performed the experiments, and analyzed data. KH, SY and KS prepared the manuscript. All authors read and approved the final manuscript.

References
1. Temple S: **The development of neural stem cells.** *Nature* 2001, **414**:112–117.
2. Sauvageot CM, Stiles CD: **Molecular mechanisms controlling cortical gliogenesis.** *Curr Opin Neurobiol* 2002, **12**:244–249.
3. Miller FD, Gauthier AS: **Timing is everything: making neurons versus glia in the developing cortex.** *Neuron* 2007, **54**:357–369.
4. Mason S, Piper M, Gronostajski RM, Richards LJ: **Nuclear factor one transcription factors in CNS development.** *Mol Neurobiol* 2009, **39**:10–23.
5. das Neves L, Duchala CS, Tolentino-Silva F, Haxhiu MA, Colmenares C, Macklin WB, Campbell CE, Butz KG, Gronostajski RM, Godinho F: **Disruption of the murine nuclear factor I-A gene (Nfia) results in perinatal lethality, hydrocephalus, and agenesis of the corpus callosum.** *Proc Natl Acad Sci USA* 1999, **96**:11946–11951.
6. Zhang W, Yi MJ, Chen X, Cole F, Krauss RS, Kang JS: **Cortical thinning and hydrocephalus in mice lacking the immunoglobulin superfamily member CDO.** *Mol Cell Biol* 2006, **26**:3764–3772.
7. Yagi S, Hirabayashi K, Sato S, Li W, Takahashi Y, Hirakawa T, Wu G, Hattori N, Hattori N, Ohgane J, Tanaka S, Liu XS, Shiota K: **DNA methylation profile of tissue-dependent and differentially methylated regions (T-DMRs) in mouse promoter regions demonstrating tissue-specific gene expression.** *Genome Res* 2008, **18**:1969–1978.
8. Kremenskoy M, Kremenska Y, Ohgane J, Hattori N, Tanaka S, Hashizume K, Shiota K: **Genome-wide analysis of DNA methylation status of CpG islands in embryoid bodies, teratomas, and fetuses.** *Biochem Biophys Res Commun* 2003, **311**:884–890.
9. Hattori N, Nishino K, Ko Y, Ohgane J, Tanaka S, Shiota K: **Epigenetic control of mouse Oct-4 gene expression in embryonic stem cells and trophoblast stem cells.** *J Biol Chem* 2004, **279**:17063–17069.
10. Nishino K, Hattori N, Tanaka S, Shiota K: **DNA methylation-mediated control of Sry gene expression in mouse gonadal development.** *J Biol Chem* 2004, **279**:22306–22313.
11. Hattori N, Imao Y, Nishino K, Ohgane J, Yagi S, Tanaka S, Shiota K: **Epigenetic regulation of Nanog gene in embryonic stem and trophoblast stem cells.** *Genes Cells* 2007, **12**:387–396.
12. Sakamoto H, Kogo Y, Ohgane J, Hattori N, Yagi S, Tanaka S, Shiota K: **Sequential changes in genome-wide DNA methylation status during adipocyte differentiation.** *Biochem Biophys Res Commun* 2008, **366**:360–366.
13. Maeda C, Sato S, Hattori N, Tanaka S, Yagi S, Shiota K: **DNA hypomethylation circuit of the mouse oocyte-specific histone H1foo gene in female germ cell lineage.** *Biol Reprod* 2008, **78**:816–821.
14. Khulan B, Thompson RF, Ye K, Fazzari MJ, Suzuki M, Stasiek E, Figueroa ME, Glass JL, Chen Q, Montagna C, Hatchwell E, Selzer RR, Richmond TA, Green RD, Melnick A, Greally JM: **Comparative isoschizomer profiling of cytosine methylation: the HELP assay.** *Genome Res* 2006, **16**:1046–1055.
15. Rakyan VK, Down TA, Thorne NP, Flicek P, Kulesha E, Gräf S, Tomazou EM, Bäckdahl L, Johnson N, Herberth M, Howe KL, Jackson DK, Miretti MM, Fiegler H, Marioni JC, Birney E, Hubbard TJ, Carter NP, Tavaré S, Beck S: **An integrated resource for genome-wide identification and analysis of human tissue-specific differentially methylated regions (tDMRs).** *Genome Res* 2008, **18**:1518–1529.
16. Hatada I, Namihira M, Morita S, Kimura M, Horii T, Nakashima K: **Astrocyte-specific genes are generally demethylated in neural precursor cells prior to astrocytic differentiation.** *PLoS One* 2008, **3**:e3189.
17. Mohn F, Weber M, Rebhan M, Roloff TC, Richter J, Stadler MB, Bibel M, Schübeler D: **Lineage-specific polycomb targets and de novo DNA methylation define restriction and potential of neuronal progenitors.** *Mol Cell* 2008, **30**:755–766.
18. Meissner A, Mikkelsen TS, Gu H, Wernig M, Hanna J, Sivachenko A, Zhang X, Bernstein BE, Nusbaum C, Jaffe DB, Gnirke A, Jaenisch R, Lander ES: **Genome-scale DNA methylation maps of pluripotent and differentiated cells.** *Nature* 2008, **454**:766–770.
19. Hirabayashi Y, Gotoh Y: **Epigenetic control of neural precursor cell fate during development.** *Nat Rev Neurosci* 2010, **11**:377–388.
20. Sato S, Yagi S, Arai Y, Hirabayashi K, Hattori N, Iwatani M, Okita K, Ohgane J, Tanaka S, Wakayama T, Yamanaka S, Shiota K: **Genome-wide DNA methylation profile of tissue-dependent and differentially methylated regions (T-DMRs) residing in mouse pluripotent stem cells.** *Genes Cells* 2010, **15**:607–618.
21. Johnson WE, Li W, Meyer CA, Gottardo R, Carroll JS, Brown M, Liu XS: **Model-based analysis of tiling-arrays for ChIP-chip.** *Proc Natl Acad Sci USA* 2006, **103**:12457–12462.
22. Shiota K: **DNA methylation profiles of CpG islands for cellular differentiation and development in mammals.** *Cytogenet Gennome Res* 2004, **105**:325–334.
23. Irizarry RA, Ladd-Acosta C, Wen B, Wu Z, Montano C, Onyango P, Cui H, Gabo K, Rongione M, Webster M, Ji H, Potash JB, Sabunciyan S, Feinberg AP: **The human colon cancer methylome shows similar hypo- and hypermethylation at conserved tissue-specific CpG island shores.** *Nat Genet* 2009, **41**:178–186.

24. Fazzari MJ, Greally JM: **Epigenomics: beyond CpG islands.** *Nat Rev Genet* 2004, **5**:446–455.
25. Yagi S, Hirosawa M, Shiota K: **DNA methylation profile: a composer-, conductor-, and player-orchestrated Mammalian genome consisting of genes and transposable genetic elements.** *J Reprod Dev* 2012, **58**:265–273.
26. Hutnick LK, Golshani P, Namihira M, Xue Z, Matynia A, Yang XW, Silva AJ, Schweizer FE, Fan G: **DNA hypomethylation restricted to the murine forebrain induces cortical degeneration and impairs postnatal neuronal maturation.** *Hum Mol Genet* 2009, **18**:2875–2888.
27. Xu GL, Bestor TH, Bourc'his D, Hsieh CL, Tommerup N, Bugge M, Hulten M, Qu X, Russo JJ, Viegas-Péquignot E: **Chromosome instability and immunodeficiency syndrome caused by mutations in a DNA methyltransferase gene.** *Nature* 1999, **402**:187–191.
28. Amir RE, Van den Veyver IB, Wan M, Tran CQ, Francke U, Zoghbi HY: **Rett syndrome is caused by mutations in X-linked MECP2, encoding methyl-CpG-binding protein 2.** *Nat Genet* 1999, **23**:185–188.
29. O'Driscoll M, Cerosaletti KM, Girard PM, Dai Y, Stumm M, Kysela B, Hirsch B, Gennery A, Palmer SE, Seidel J, Gatti RA, Varon R, Oettinger MA, Neitzel H, Jeggo PA, Concannon P: **DNA ligase IV mutations identified in patients exhibiting developmental delay and immunodeficiency.** *Mol Cell* 2001, **8**:1175–1185.
30. Lu W, Quintero-Rivera F, Fan Y, Alkuraya FS, Donovan DJ, Xi Q, Turbe-Doan A, Li QG, Campbell CG, Shanske AL, Sherr EH, Ahmad A, Peters R, Rilliet B, Parvex P, Bassuk AG, Harris DJ, Ferguson H, Kelly C, Walsh CA, Gronostajski RM, Devriendt K, Higgins A, Ligon AH, Quade BJ, Morton CC, Gusella JF, Maas RL: **NFIA haploinsufficiency is associated with a CNS malformation syndrome and urinary tract defects.** *PLoS Genet* 2007, **3**:e80.
31. Frank KM, Sharpless NE, Gao Y, Sekiguchi JM, Ferguson DO, Zhu C, Manis JP, Horner J, DePinho RA, Alt FW: **DNA ligase IV deficiency in mice leads to defective neurogenesis and embryonic lethality via the p53 pathway.** *Mol Cell* 2000, **5**:993–1002.
32. Deuel TA, Liu JS, Corbo JC, Yoo SY, Rorke-Adams LB, Walsh CA: **Genetic interactions between doublecortin and doublecortin-like kinase in neuronal migration and axon outgrowth.** *Neuron* 2006, **49**:41–53.
33. Demyanenko GP, Riday TT, Tran TS, Dalal J, Darnell EP, Brennaman LH, Sakurai T, Grumet M, Philpot BD, Maness PF: **NrCAM deletion causes topographic mistargeting of thalamocortical axons to the visual cortex and disrupts visual acuity.** *J Neurosci* 2011, **31**:1545–1558.
34. Ohgane J, Wakayama T, Kogo Y, Senda S, Hattori N, Tanaka S, Yanagimachi R, Shiota K: **DNA methylation variation in cloned mice.** *Genesis* 2001, **30**:45–50.
35. Arai Y, Ohgane J, Yagi S, Ito R, Iwasaki Y, Saito K, Akutsu K, Takatori S, Ishii R, Hayashi R, Izumi S, Sugino N, Kondo F, Horie M, Nakazawa H, Makino T, Shiota K: **Epigenetic assessment of environmental chemicals detected in maternal peripheral and cord blood samples.** *J Reprod Dev* 2011, **57**:507–517.
36. Maekawa R, Yagi S, Ohgane J, Yamagata Y, Asada H, Tamura I, Sugino N, Shiota K: **Disease-dependent differently methylated regions (D-DMRs) of DNA are enriched on the X chromosome in uterine leiomyoma.** *J Reprod Dev* 2011, **57**:604–612.
37. Lieb JD, Beck S, Bulyk ML, Farnham P, Hattori N, Henikoff S, Liu XS, Okumura K, Shiota K, Ushijima T, Greally JM: **Applying whole-genome studies of epigenetic regulation to study human disease.** *Cytogenet Genome Res* 2006, **114**:1–15.
38. Jones PA, Baylin SB: **The epigenomics of cancer.** *Cell* 2007, **128**:683–692.
39. Smedley D, Haider S, Ballester B, Holland R, London D, Thorisson G, Kasprzyk A: **BioMart–biological queries made easy.** *BMC Genomics* 2009, **10**:22.
40. Giardine B, Riemer C, Hardison RC, Burhans R, Elnitski L, Shah P, Zhang Y, Blankenberg D, Albert I, Taylor J, Miller W, Kent WJ, Nekrutenko A: **Galaxy: a platform for interactive large-scale genome analysis.** *Genome Res* 2005, **15**:1451–1455.
41. Saeed AI, Sharov V, White J, Li J, Liang W, Bhagabati N, Braisted J, Klapa M, Currier T, Thiagarajan M, Sturn A, Snuffin M, Rezantsev A, Popov D, Ryltsov A, Kostukovich E, Borisovsky I, Liu Z, Vinsavich A, Trush V, Quackenbush J: **TM4: a free, open-source system for microarray data management and analysis.** *Biotechniques* 2003, **34**:374–378.
42. Huang Da W, Sherman BT, Tan Q, Kir J, Liu D, Bryant D, Guo Y, Stephens R, Baseler MW, Lane HC, Lempicki RA: **DAVID bioinformatics resources: expanded annotation database and novel algorithms to better extract biology from large gene lists.** *Nucleic Acids Res* 2007, **35**(Web Server issue):W169–W175.
43. Sim FJ, McClain CR, Schanz SJ, Protack TL, Windrem MS, Goldman SA: **CD140a identifies a population of highly myelinogenic, migration-competent and efficiently engrafting human oligodendrocyte progenitor cells.** *Nat Biotechnol* 2011, **29**:934–941.